

## Research Article

## Effect of Processing Parameters on the Morphology of $\alpha$ -phase in Ti-6Al-4V Alloy During the Two-step Hot Deformation

H.R. Ezatpour<sup>1\*</sup>, G.R. Ebrahimi<sup>2\*</sup> and F. Zarghani<sup>3</sup><sup>1</sup> Department of Engineering Sciences, Hakim Sabzevari University, Sabzevar, Iran<sup>2</sup> Department of Materials Science and Metallurgical Engineering, Engineering Faculty, Ferdowsi University of Mashhad, Mashhad, Iran<sup>3</sup> Department of Materials and Polymer Engineering, Hakim Sabzevari University, Sabzevar, Iran

## ARTICLE INFO

*Article history:*

Received 09 December 2023

Reviewed 10 January 2024

Revised 23 January 2024

Accepted 27 January 2024

*Keywords:*

Ti-6Al-4V alloy

Two-step hot deformation process

Microstructure

*Please cite this article as:*

H.R. Ezatpour, G.R. Ebrahimi, F. Zarghani, Effect of Processing Parameters on the Morphology of  $\alpha$ -phase in Ti-6Al-4V Alloy During the Two-step Hot Deformation, *Iranian Journal of Materials Forming*, 10 (3) (2023) 54-62.

## ABSTRACT

The morphology of the  $\alpha$ -phase in titanium alloys considerably affected their physical and mechanical properties. In this research, the effect of applied strain and inter-pass times on the morphology of the  $\alpha$ -phase was studied in the two-step hot deformation process. Hot compression tests were performed at 900 °C and 0.001 s<sup>-1</sup> while the strains in the first and second passes were set as (first cycle: 0.6 and 0.3) and (second cycle: 0.3 and 0.6) respectively, with various inter-pass times. The work softening parameter obtained from the stress-strain curves showed that the proper time for globularization of  $\alpha$ -layers for the first pass strain of 0.6 was 240 s and for the second strain of 0.3 it was 240 and 300 s. Microstructure results indicated that the first pass strain of 0.3 and the inter-pass time of 240 s were the optimum conditions for globularization of  $\alpha$  layers.

© Shiraz University, Shiraz, Iran, 2023

### 1. Introduction

Due to high strength, low density, low modulus (high ductility), high resistance to corrosion and remarkable compatibility for in-vivo applications, titanium and its alloys have been considered as one of the most interesting subjects in different applications [1, 2]. In recent years, Ti-6Al-4V (Ti-64) alloys have been used

instead of commercially pure titanium due to their high strength and reasonable toughness [3]. In this field, many attempts have been made to develop titanium alloys for use for medical uses such as implants [4, 5]. Therefore, one of the main goals is to improve the mechanical properties of the titanium alloys. Many researchers have focused on the effects of hot deformation parameters such as the strain, strain rate,

\* Corresponding authors

E-mail address: [h.ezatpour@hsu.ac.ir](mailto:h.ezatpour@hsu.ac.ir) (H.R. Ezatpour),E-mail address: [r.ebrahimi@um.ac.ir](mailto:r.ebrahimi@um.ac.ir) (G. R. Ebrahimi)<https://doi.org/10.22099/IJMF.2024.49049.1277>

temperature, and heat treatment on the morphology optimization of  $\alpha$ -phase of Ti-64 alloy which is one of the most significant aspects of this alloy [6-8]. Recent research has demonstrated that titanium alloys with a homogeneous distribution of globularized  $\alpha$ -phase in  $\beta$  matrix presents suitable mechanical and physical properties like high strength, low density, and high corrosion resistance [9, 10].

Kim et al. [6] investigated the quantity and quality of globularized  $\alpha$ -phase as well as the alloy microstructural changes caused by the multi-step hot deformation process in the Ti-64 alloy. They examined the globularized phenomenon of  $\alpha$  layers under the deformation process by measuring the aspect ratio (L/D ratio: L and D are the length and the width of  $\alpha$ -layers, respectively) and the size of  $\alpha$ -layers. Based on their results, thinner layers of  $\alpha$ -phase easily changed their morphology to a globularized state. Zhang et al. [11] explored globularization mechanisms in Ti alloys such as bending, breaking up, and separating of  $\alpha$  layers. Dutta et al. [12] investigated microstructure changes of the Ti-64 alloy under multi-step hot deformation. According to their experiments, the speed of the softening phenomenon decreased by increasing the deformation temperature. Zherebtsov et al. [13] studied the effect of initial microstructure and hot deformation parameters on the microstructure properties of titanium commercial alloys. Accordingly, the initial martensitic microstructure considerably affected the formation of globularized and homogeneous microstructures. Kim et al. [14] considered the effect of  $\alpha$ -phase layer thickness on the amount of globularization by two different heat treatments that took place before the deformation process. Stefansson et al. [15] studied the microstructure evolution of Ti-64 alloy from lamellar to equiaxed morphologies by the hot deformation process. They concluded that the amount of globularized  $\alpha$ -phase increases by the increment of the amount of strain and annealing heat treatment time. Warchomicka et al. [16] also studied the effects of heat treatment and hot deformation parameters on the microstructure of Ti-64 alloy through hot compression tests and achieved the same results. He et al. [17] showed a grain refining

structure in the alloy by the microstructural changes under hot deformation and phase transformation. Ding et al. [9] indicated that the microstructure of Ti-6Al-4V alloy is extremely under the influence of initial microstructure, hot working temperature, strain, strain rate, and also the cooling rate during hot compression tests. Zhang et al. [18] studied the effect of initial microstructure on hot deformation behavior and microstructure evolution of Ti-64 alloy. They confirmed that the globularization of  $\alpha$  phase at a low strain rate and the formation of shear bands at a high strain rate are the main mechanisms of microstructure evolutions taking place during deformation.

Based on the literature, determining the optimal parameters for the removal of lamellar  $\alpha$ -phase structure and achieving a globularized structure in titanium alloys is very significant. Therefore, the current work aim is to examine the effect of deformation parameters on the microstructure of Ti-64 alloy during the two-step hot deformation process to determine appropriate conditions to obtain a globularized microstructure.

## 2. Experimental Procedure

Ti-64 alloy was used as the initial material with a chemical composition, as reported in Table 1. All the samples were prepared with a length and diameter of 15 mm and 10 mm, respectively, from the rod with a diameter of 16 mm. Hot compression tests were performed by using a Zwick-Roell 250 universal testing machine equipped with a resistance furnace with a temperature control precision of  $\pm 5$  °C. The samples were kept for 3 min at the deformation temperature to avoid any temperature gradient. Moreover, Mica sheets were used as a lubricant during process.

**Table 1.** Chemical composition of Ti-6Al-4V alloy used in this study

Elements	Al	V	Si	Zr	Fe	C	O	N	Ti
Wt.%	6.3	4.1	0.03	0.02	0.18	0.01	0.018	0.01	base

Samples Fig. 1 shows a schematic illustration of the two-step hot deformation process with the first pass strains of 0.6 and 0.3 and second pass strains of 0.3 (with

inter-pass times of 120, 240 and 480 s) and 0.6 (inter-pass times of 240, 300 and 500 s), respectively. In all cycles, the hot deformation temperature and strain rate were set as 900 °C and 0.001 s<sup>-1</sup>, respectively. Due to the higher level of the first pass strain in the first cycle (Fig. 1 (a)), the periods between deformation steps were shorter. The appropriate strain rate in tests was selected based on the globularization process of  $\alpha$ -phase via  $\beta$ -phase diffusion rate into created borders in  $\alpha$ -layers. At high temperatures and low strain rates, the volume fraction of the globularized  $\alpha$ -phase is increased due to suitable conditions for migration of lamellar structures by diffusion [8, 19, 20]. Furthermore, it has been reported that the hot compression tests applied in the temperature range of  $\beta$ + $\alpha$  two phases (800-975 °C) results in a better globularized  $\alpha$ -phase [21-26].

Samples were sectioned by wire cut parallel to the axis of pressure to examine the microstructure. A (a) ion containing 6% HNO<sub>3</sub>, 2% HF, and 92% H<sub>2</sub>O was used as etchant. Microstructural images were taken using Optical Microscopy (Olympus-GX51) and Scanning Electron Microscopy (SEM) in different conditions.

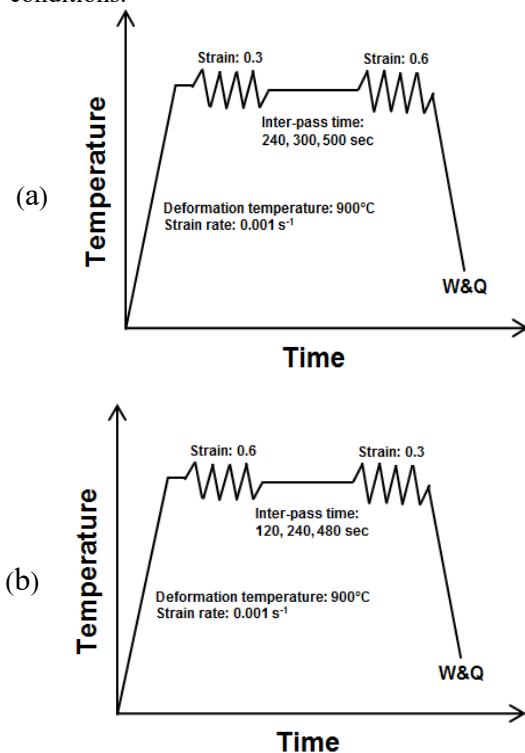


Fig. 1. Schematic illustration of the two-step hot deformation process with the first pass strains of (a) 0.6 and (b) 0.3 and various inter-pass times.

### 3. Results and Discussion

Initial microstructure of Ti-64 alloy is shown in Fig. 2 (a). The suitable microstructure for deformation should be martensitic. Therefore, the alloy was heated up to the temperature of 1020 °C (temperature range of  $\beta$ -single phase) with a holding time of 30 min and then quenched in water (Fig. 2 (b)). The grain size of  $\beta$  phase after the heat treatment was measured at about 87  $\mu$ m.

The true stress-strain curves of Ti-64 alloy at the temperature of 900 °C and strain rate of 0.001 s<sup>-1</sup> during the two-step deformation process are shown in Fig. 3 (a, b). In all curves, flow stress presents a peak in low strains. By increasing the amount of strain, the softening phenomenon occurs and the stress level decreases. The curves can be divided into three sections: Firstly, the stress level rises quickly because of the hardening phenomenon during the deformation process. The second section is commenced by slowing down the work hardening and the occurrence of work softening and the creation of dislocation-free grains by microstructural changes [12, 20]. Thermally activated processes control microstructural changes and morphology of phases. In this step, the decrement of hardening continues until it reaches zero. As a result, competition between the hardening and softening phenomena creates a peak in the true stress-strain curves. In the third section, the rate of the softening phenomena decreases until the level of stress reaches a stable value and the rate of hardening is equal to the rate of softening called the steady state region [27-33].

In addition, there are instabilities or serrations in all the curves due to adiabatic conditions during deformation. During hot deformation, the low thermal conductivity of the Ti-64 alloy leads to temperature rising in some regions because the produced heat is not easily able to transfer through other parts of the sample; so it creates the localized reduction of flow stress during the process [29, 34]. Moreover, in the two-step deformation process, the required stress for starting the second stage increases by incrementing the inter-pass times which can be attributed to the delay in dynamic globularization by increasing the thickness of  $\alpha$  layers

[29, 30]. For analyzing the true stress-strain curves in the two-step deformation, the softening parameter (S) can be defined. This parameter is defined as the ratio of maximum ( $\sigma_i$ ) to minimum amount ( $\sigma_s$ ) of stress, and it is directly related to microstructure evolutions. The higher amount of S parameter indicates that the microstructure is mainly affected by globularized  $\alpha$ -layers. The values of S parameter for three different time periods and the first pass strains of 0.6 and 0.3 are reported in Tables 2 and 3, respectively. Based on the results and the highest value of the softening parameter, the most appropriate time for globularization of  $\alpha$ -layers for the first pass strain of 0.6 is 240 s and for 0.3 it is 240 and 300 s.

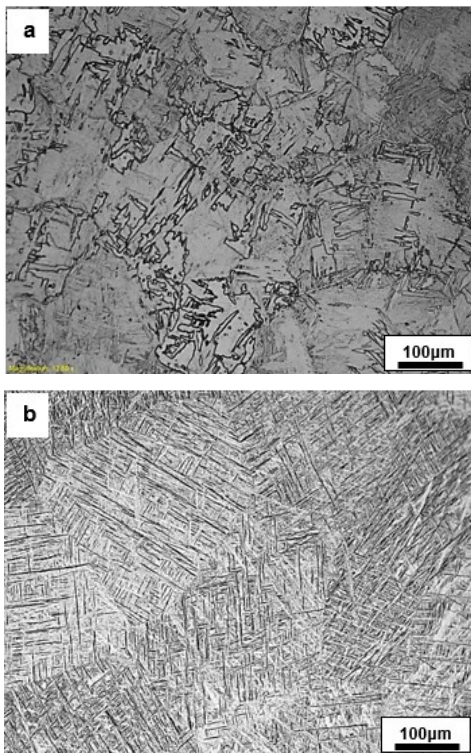


Fig. 2. Optical microstructures of Ti-64 alloy (a) as-received, (b) after treatment at 1020 °C for 30 min, quenched in water.

Table 2. Maximum and minimum true stresses and softening parameter in the two-step compression tests of Ti-64 alloy on the first pass strain of 0.6

Time (s)	120		240		480	
	$\sigma_i$	$\sigma_s$	$\sigma_i$	$\sigma_s$	$\sigma_i$	$\sigma_s$
True stress (MPa)	14.9	13.8	16.4	12.9	17.4	14.9
Softening parameter	1.07		1.27		1.17	

Table 2. Maximum and minimum true stresses and softening parameter in the two-step compression tests of Ti-64 alloy in the first pass strain of 0.3

Time (s)	120		240		480	
	$\sigma_i$	$\sigma_s$	$\sigma_i$	$\sigma_s$	$\sigma_i$	$\sigma_s$
True stress (MPa)	17.2	8.9	20.8	10.4	19	11.2
Softening parameter	1.93		2		1.70	

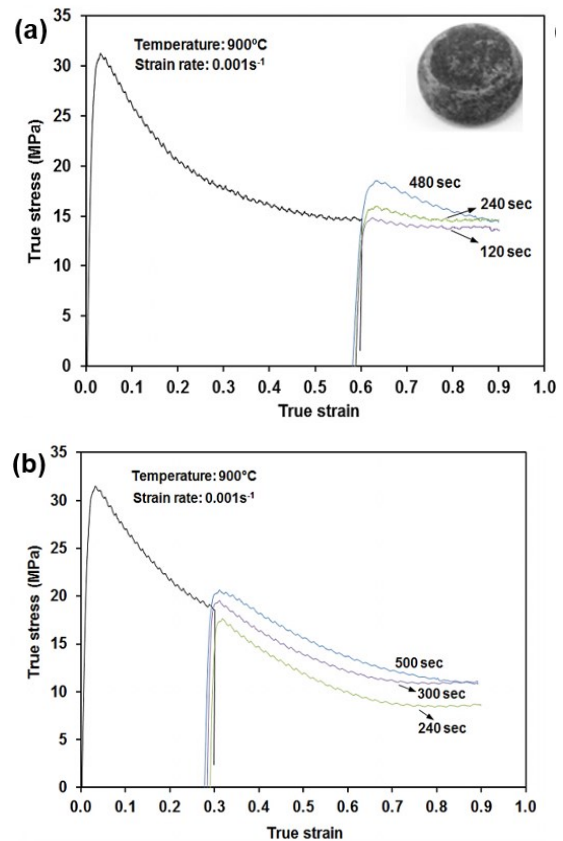


Fig. 3. Two-step true stress-strain curves obtained at 900 °C and 0.001 s<sup>-1</sup> and various inter-pass times of (a) the first cycle, (b) the second cycle.

A macroscopic image of the deformed sample of Ti-64 alloy at 900 °C and strain rate of 0.001 s<sup>-1</sup> is illustrated in Fig. 4. As can be seen from the image, the deformed microstructure can be divided into three areas including (1) the area without deformation, (2) the area which is partially deformed under tensile stress and (3) the highly deformed area which is under the shear stress.

Fig. 5 presents the microstructures of different zones shown in Fig. 4. In the area without deformation,  $\alpha$  phase morphology has no change and neither do lamellar and martensitic (Fig. 5 (a)). In the partial deformation zone (Fig. 5 (b)), although many changes in the



morphology of  $\alpha$  phase have occurred, this phase is still observed as a lamellar structure through many parts of the sample. This microstructure is called “Bimodal” microstructure. In the third zone (Fig. 5 (c)), the effect of strain is enough to break down  $\alpha$  layers and change their morphology from lamellar to globularization. Thus, dynamic globularization is observed in the second and third zones. In these zones,  $\alpha$  layers orient in the perpendicular direction of the applied strain axis.

In the two-step deformation process, one of the most significant factors is the inter-pass time. Inter-pass time can be directly related to  $\alpha$  layer thickness [14]. The microstructure images of deformed Ti-64 alloy and details according to the first cycle and various inter-pass times (Fig. 2 (a)) are illustrated in Fig. 6 and Table 2. According to Fig. 6(a), the applied stress during deformation causes remarkable changes in the morphology of  $\alpha$  layers. By increasing the inter-pass time of deformation up to 240 s, the volume fraction of  $\alpha$ -phase has not noticeably changed, but on the other hand, the size and aspect ratio of these layers have decreased (Fig. 6 (b)). Therefore, the amount of globularized  $\alpha$  phase has increased by increasing the inter-pass time. With further increase of inter-pass time up to 480 s (Fig. 6 (c)), the size and continuity of  $\alpha$  layers have increased. It is noteworthy to mention that by holding the sample in deformation temperature, the thickness of  $\alpha$  layers increases which leads to a proportional increase of the required stress value for separating and squeezing the layers. Furthermore, the strain of 0.3 in the second step is not sufficient for splitting these layers. Moreover,  $\beta$ -phase diffusion into thicker layers of  $\alpha$  phase for globularization is more difficult.

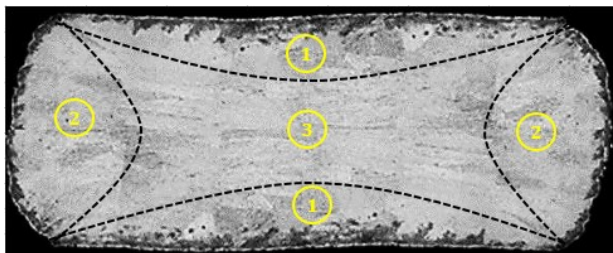


Fig. 4. Macroscopic image of the deformed sample of Ti-64 alloy at 900 °C and strain rate of 0.001 s<sup>-1</sup>.

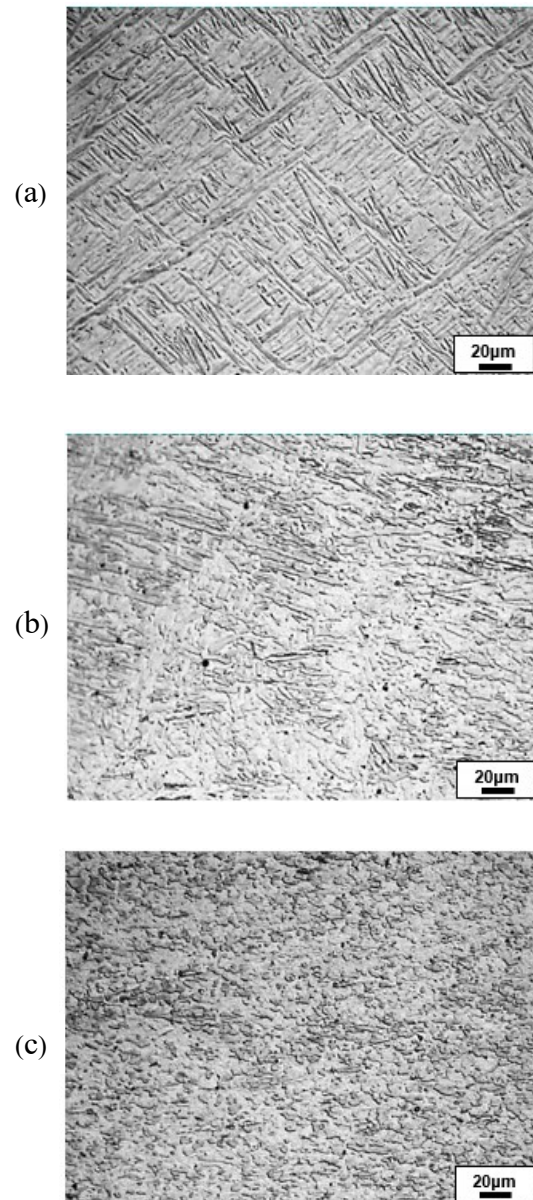


Fig. 5. (a) Microstructures of Ti-64 alloy after hot deformation at 900 °C and strain rate of 0.001 s<sup>-1</sup> at different zone of “1”, (b) zone “2”, (c) zone “3”.

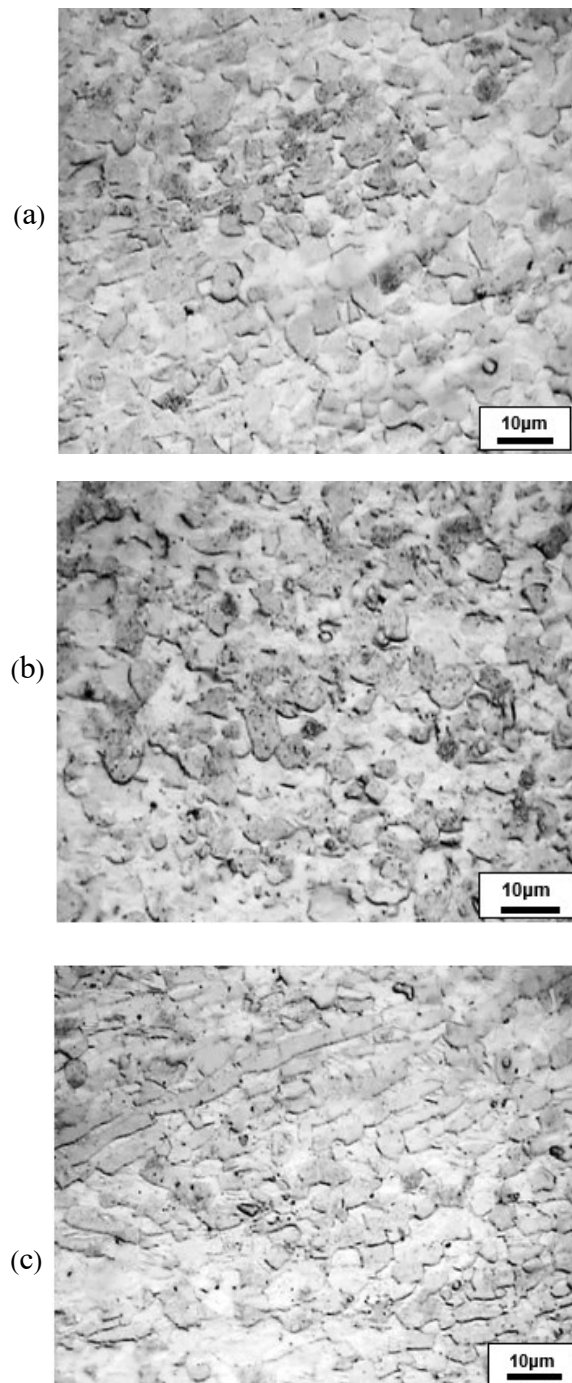
Consequently, by increasing the inter-pass time, the change of morphology from lamellar to globularization becomes more difficult.

Fig. 7 and Table 3 show the microstructures and details of the Ti-64 alloy after the two-step hot deformation in the first strain pass of 0.3 (Fig. 2 (b)). At 240 s (Fig. 7 (a)), the volume fraction of  $\alpha$  phase and aspect ratio are smaller than 300 s (Fig. 7 (b)). At 500 s (Fig. 7 (c)), the  $\beta$  phase has the appropriate opportunity to penetrate the boundaries of  $\alpha$  phase. Nevertheless, the size of  $\alpha$  layers in this condition is bigger than 240 s. Consequently, the fracture of layers is more difficult in

this condition. In addition, the size, volume fraction and aspect ratio of  $\alpha$  layers in the strain of 0.3 is smaller than strain of 0.6 (Fig. 6). In general, deformation under an initial strain of 0.3 provides more suitable conditions for the globularization of layers. As explained, by holding the sample in inter-pass period, the thickness of  $\alpha$ -layers increases. Therefore, the diffusion of  $\beta$ -phase into layers is more difficult and the globularization process needs more strain. Therefore, the strain of 0.3 in the second step is inadequate for splitting and separating the layers.

The globularization mechanism of  $\alpha$  phase morphology is shown in Fig. 8. Fig. 8 (a) illustrates that some  $\alpha$  layers (dark color phase) are in wave form with bending changes which are one of the starting mechanisms of globularization. This mechanism includes splitting and separating  $\alpha$  layers by using shear stress during the process (Fig. 8 (b)) which is controlled by the rate of  $\beta$ -phase diffusion into the separated regions. Similar results have been reported by the others [21, 35, 36]. By increasing the temperature and decreasing the strain rate, the rate of diffusion increases, and separation takes place more easily [37-39]. Weiss et al. [40], Park et al. [30] and Seshacharyulu et al. [41] believed that the crushing  $\alpha$ -layers is due to the bending layers under applied shear stress and also the creation of

sub-grain boundaries in these layers. Semiatin et al. [42] have also reported the initiation of dynamic globularization of the twisted parts of these layers.



**Fig. 6.** Optical microstructure of Ti-64 alloy deformed at 900 °C and  $0.001\text{s}^{-1}$  and the first pass strain of 0.6, second pass strain of 0.3 and inter-pass times of (a) 120, (b) 240, (c) 480 s.

**Table 3.** Grain size, volume fraction and aspect ratio of  $\alpha$  phase based on analyzing microstructure images from Fig. 6

The first cycle	Time (s)	$\alpha$ grain size ( $\mu\text{m}$ )	Volume fraction of $\alpha$ phase (%)	Aspect ratio of $\alpha$ phase
1	120	18	62	3.5
2	240	14	62.5	2.5
3	480	26	66	4

**Table 4.** Grain size, volume fraction and aspect ratio of  $\alpha$  phase based on analyzing microstructure images from Fig. 7

The second cycle	Time (s)	$\alpha$ grain size ( $\mu\text{m}$ )	Volume fraction of $\alpha$ phase (%)	Aspect ratio of $\alpha$ phase
1	240	14	40.5	1.5
2	300	18	61	2.4
3	500	15	71	3.3



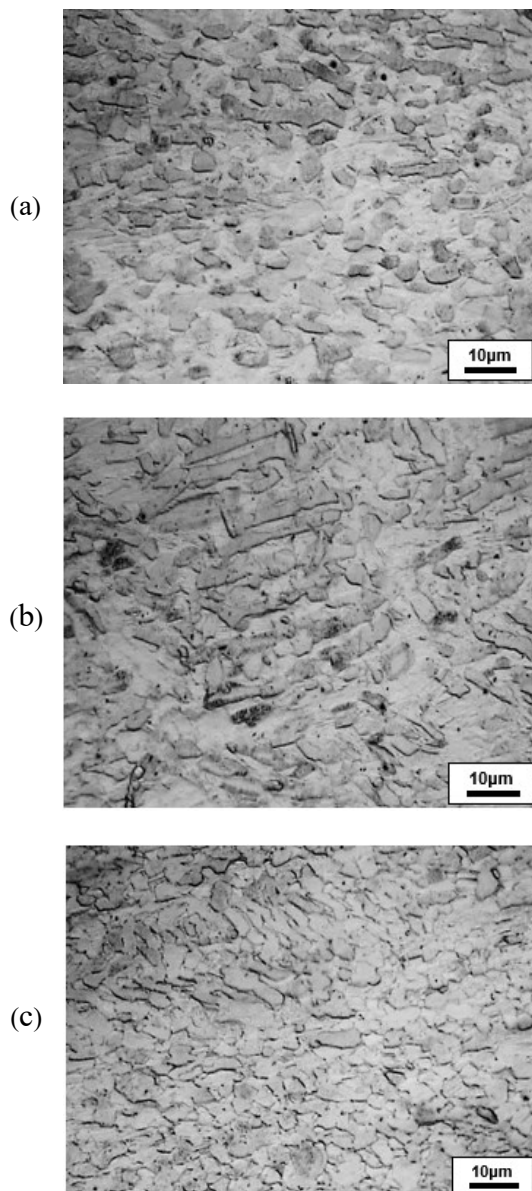


**Fig. 7.** Optical microstructure of Ti-64 alloy deformed at 900 °C and  $0.001\text{s}^{-1}$  and the first pass strain of 0.3, second pass strain of 0.6 with inter-pass times (a) 240, (b) 300, (c) 500 s.

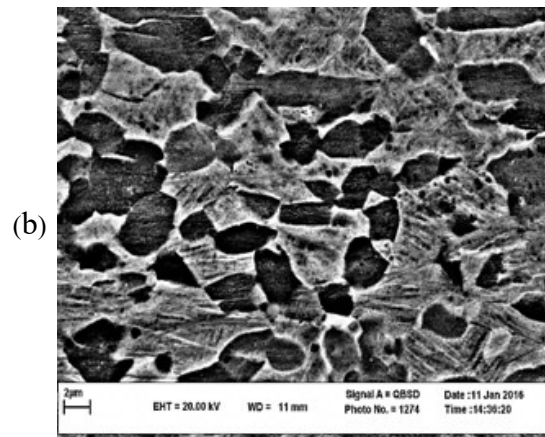
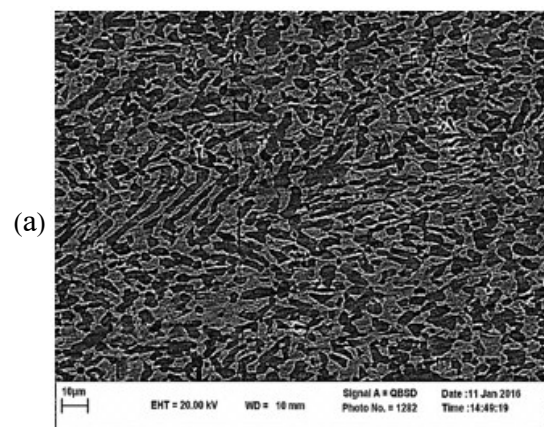


**Fig. 8.** SEM micrographs of hot deformed Ti-64 alloy showing the splitting and globularization of  $\alpha$  phase.

#### 4. Conclusion

In this work, the two-step hot deformation process was designed to investigate the effect of the first and second strains and inter-pass times on the morphology of  $\alpha$  phase of Ti-64 alloy. The following conclusions were achieved:

1. In the two-step deformation process, the required stress for starting the second stage was increased with the increment of the inter-pass time due to the delay in dynamic globularization.
2. The softening parameter indicated that the appropriate time for globularization of  $\alpha$ -layers for the first pass strain of 0.6 is 240 s, and for 0.3 is 240 and 300 s.
3. Microstructure results showed that the first pass strain of 0.3 and inter-pass time of 240 s were the optimum conditions for the globularization of  $\alpha$  layers.

#### Conflict of Interests

The authors have no conflicts of interest to declare.

#### Funding

This research has not received any specific fund to be declared here.

## 5. References

- [1] L. Shao, W. Li, D. Li, G. Xie, C. Zhang, C. Zhang, J. Huang, A review on combustion behavior and mechanism of Ti alloys for advanced aero-engine, *J. Alloys Compd.*, 960 (2023).
- [2] J. Wang, K. Wang, S. Lu, X. Li, D. OuYang, and Q. Qiu, Softening mechanism and process parameters optimization of Ti-4.2Al-0.005B titanium alloy during hot deformation, *J. Mater. Res. Technol.*, 17 (2022) 1842-1851.
- [3] K. Prasad, H. Krishnaswamy, N. Arunachalam, Investigations on ductility improvement and reloading yielding during stress relaxation of dual phase Ti-6Al-4V titanium alloy, *J. Alloys Compd.*, 828 (2020).
- [4] C. N. Elias, J. H. C. Lima, R. Valiev, and M. A. Meyers, Biomedical Applications of Titanium and its Alloys, *Bio. Mater. Sci.* 60 (2008) 46-9.
- [5] M. Niinomi, Biologically and Mechanically Biocompatible Titanium Alloys, *Mater. Trans.*, 49 (2008) 2170-2178.
- [6] J. Y. Kim, K.-T. Park, I. O. Shim, S. H. Hong, Globularization Behavior of ELI Grade Ti-6Al-4V Alloy during Non-Isothermal Multi-Step Forging, *Mater. Trans.*, 49 (2008) 215-223.
- [7] J. Luo, M. Li, H. Li, W. Yu, Effect of the strain on the deformation behavior of isothermally compressed Ti-6Al-4V alloy, *Mater. Sci. Eng. A.*, 505 (2009) 88-95.
- [8] C.H. Park, K.T. Park, D.H. Shin, C.S. Lee, Microstructural mechanisms during dynamic globularization of Ti-6Al-4V Alloy, *Mater. Trans.*, 49 (2008) 2196-2200.
- [9] R. Ding, Z. X. Guo, A. Wilson, Microstructural evolution of a Ti-6Al-4V alloy during thermomechanical processing, *Mater. Sci. Eng. A.*, 327 (2002) 233-245.
- [10] G. Lütjering, J. C. Williams, Titanium, Springer, vol. 2, (2007).
- [11] J. Zhang, H. Li, and M. Zhan, Review on globularization of titanium alloy with lamellar colony, *Manuf. Rev.*, 18 (2020) 1-14.
- [12] J. B. A. Dutta, A. Kumar, T. Raghu, Flow behaviour of Ti-6Al-4V subjected to Step temperature isothermal forging, *Int. J. Technol. Adv. Eng.*, 2 (2012) 321-325.
- [13] S.V. Zherebtsov, G.A. Salishchev, R.M. Galeyev, O.R. Valiakhetov, S.Yu. Mironov, S.L. Semiatin, Production of submicrocrystalline structure in large-scale Ti-6Al-4V billet by warm severe deformation processing, *Scr. Mater.*, 51 (2004) 1147-1151.
- [14] J. Y. Kim, I. O. Shim, S. H. Hong, Effect of Initial Lamellar Structure on Globularization of Hot Multi-Forged ELI Grade Ti-6Al-4V Alloy, *Mater. Sci. Forum.*, (2007).
- [15] S. L. Semiatin, N. Stefansson, R. D. Doherty, Prediction of the kinetics of static globularization of Ti-6Al-4V, *Metall. Mater. Trans. A*, 36 (2005) 1372-1376.
- [16] F. Warchomicka, C. Poletti, M. Stockinger, T. Henke, Microstructure evolution during hot deformation of Ti-6Al-4V double cone specimens, *Int. J. Mater. Form.*, 3 (2010) 215-218.
- [17] L. He, A. Dehghan-Manshadi, R. J. Dippenaar, The evolution of microstructure of Ti-6Al-4V alloy during concurrent hot deformation and phase transformation, *Mater. Sci. Eng. A*, 549 (2012) 163-167.
- [18] Z. X. Zhang, S. J. Qu, A. H. Feng, J. Shen, D. L. Chen, Hot deformation behavior of Ti-6Al-4V alloy: Effect of initial microstructure, *J. Alloys Compd.*, 718, (2017) 170-181.
- [19] M. Motyka, J. Sieniawski, W. Ziąja, Microstructural aspects of superplasticity in Ti-6Al-4V alloy, *Mater. Sci. Eng. A*, 599 (2014) 57-63.
- [20] J.T. Yeom, J.H. Kim, N.Y. Kim, N.K. Park, C.S. Lee, Characterization of dynamic globularization behavior during hot working of Ti-6Al-4V alloy, *Adv. Mater. Res.*, 26-28 (2007) 1033-1036.
- [21] F. Zarghani, G. R. Ebrahimi, J. Taheri, H. R. Ezatpour, Hot compressive deformation behavior of Ti-8Al-1Mo-1 V titanium alloy at elevated temperatures : Focus on flow behavior , constitutive modeling , and processing maps, *Mater. Today Commun.*, 37 (2023).
- [22] M. Arulselvan and G. Ganesan, A study on compression test on Ti-6Al-4V in various strain rates and various temperature, *Int. J. Rec. Technol. Eng. (IJRTE)*, 2 (2013) 47-51.
- [23] P. Honarmandi, M. Aghaie-Khafri, Hot deformation behavior of Ti-6Al-4V alloy in  $\beta$  phase field and low strain Rate, *Metallogr. Microstruct. Anal.*, 2 (2012) 13-20.
- [24] J. Luo, M. Li, W. Yu, H. Li, Effect of the strain on processing maps of titanium alloys in isothermal compression, *Mater. Sci. Eng. A*, 504 (2009) 90-98.
- [25] P. C. Collins, B. Welk, T. Searles, J. Tiley, J. C. Russ, H. L. Fraser, Development of methods for the quantification of microstructural features in  $\alpha + \beta$ -processed  $\alpha/\beta$  titanium alloys, *Mater. Sci. Eng. A*, 508 (2009) 174-182.
- [26] W. Yu, M. Li, J. Luo, Effect of processing parameters on microstructure and mechanical properties in high temperature deformation of Ti-6Al-4V Alloy, *Rare Met. Mater. Eng.*, 38 (2009) 19-24.
- [27] W. S. Lee, C. F. Lin, Plastic deformation and fracture behaviour of Ti6Al4V alloy loaded with high strain rate under various temperatures. *Mater. Sci. Eng. A.*, 241 (1998) 48-59.
- [28] M. A. Shafaat, H. Omidvar, B. Fallah, Prediction of hot compression flow curves of Ti-6Al-4V alloy in  $\alpha+\beta$  phase region, *Mater. Des.* , 32 (2011) 4689-4695.



- [29] S. J. Mirahmadi, M. Hamed, M. Habibi Parsa, Investigation of microstructural uniformity during isothermal forging of Ti-6Al-4V, *J. Mater. Eng. Perform.*, 23 (2014), 4411-4420.
- [30] C. H. Park, Y. G. Ko, J. W. Park, C. S. Lee, Enhanced superplasticity utilizing dynamic globularization of Ti-6Al-4V alloy, *Mater. Sci. Eng. A*, 496 (2008) 150-158.
- [31] S. Nemat-Nasser, W. G. Guo, V. F. Nesterenko, S. S. Indrakanti, Y. B. Gu, Dynamic response of conventional and hot isostatically pressed Ti-6Al-4V alloys: Experiments and modeling, *Mech. Mater.*, 33 (2001) 425-439.
- [32] H. Song, S. Zhang, M. Cheng, Dynamic globularization prediction during cogging process of large size TC11 titanium alloy billet with lamellar structure, *Def. Technol.*, 10 (2014) 40-46.
- [33] R. M. Poths, B. P. Wynne, W. M. Rainforth, J. H. Beynon, G. Angella, S. L. Semiatin, Effect of strain reversal on the dynamic spheroidization of Ti-6Al-4V during hot deformation, *Metall. Mater. Trans. A*, 35 (2004) 2993-3001.
- [34] H. Monajati, K. Taheri, M. Jahazi, S. Yue, Deformation characteristics of isothermally forged UDIMET 720 nickel-base superalloy, *Metall. Mater. Trans. A*, 36 (2005), 895-905.
- [35] C. Lin, G. Pang, Y. Jiang, X. Liu, X. Zhang, C. Chen, Hot compressive deformation behavior and microstructure evolution of a Ti-55511 alloy with basket-weave microstructures, *Vac.*, 169 (2019).
- [36] Y. C. Lin, Y. Xiao, Y. Jiang, G. Pang, H. Li, Materials Science & Engineering A Spheroidization and dynamic recrystallization mechanisms of Ti-55511 alloy with bimodal microstructures during hot compression in  $\alpha/\beta$  region, *Mater. Sci. Eng. A*, 782 (2020).
- [37] G. R. Ebrahimi, F. Zarghani, H. R. Ezatpour, M. J. Taheri, "Hot working behaviour of Ti – 8Al – 1Mo – 1V alloy through the hot compression test, *Mater. Sci. Technol.*, (2024).
- [38] M. Cabibbo, A. Di Salvia, S. Zhrebtsov, Loss of coherency at interphase  $\alpha/\beta$  boundary in Ti-6Al-4V alloys during deformation at 800°C, *La Metall. Italiana*, (2012) 29-36.
- [39] H. Matsumoto, L. Bin, S. H. Lee, Y. Li, Y. Ono, A. Chiba, Frequent occurrence of discontinuous dynamic recrystallization in Ti-6Al-4V Alloy with  $\alpha$  martensite starting microstructure, *Metall. Mater. Trans. A*, 44 (2012) 3245-3260,
- [40] I. Weiss, F. H. Froes, D. Eylon, G. E. Welsch, Modification of alpha morphology in Ti-6Al-4V by thermomechanical processing, *Metall. Trans. A*, 17 (1986) 1935-1947.
- [41] T. Seshacharyulu, S. C. Medeiros, W. G. Frazier, Y.V.R.K. Prasad, Microstructural mechanisms during hot working of commercial grade Ti-6Al-4V with lamellar starting structure, *Mater. Sci. Eng. A*, 325 (2002) 112-125.
- [42] S. Semiatin, V. Seetharaman, I. Weiss, Flow behavior and globularization kinetics during hot working of Ti-6Al-4V with a colony alpha microstructure, *Mater. Sci. Eng. A*, 263 (1999) 257-271.
- [43] P. Crook, Cobalt and Cobalt Alloys, ASM Handbook, Properties Selection of Nonferrous Alloy and Special-Purpose Material, *ASM International USA*, 1990, pp. 1416-1421.